Investigation of cohesive energy effects on size-dependent physical and chemical properties of nanocrystals

Chun Cheng Yang* and Sean Li
School of Materials Science and Engineering, The University of New South Wales, NSW 2052 Australia
(Received 14 November 2006; revised manuscript received 2 March 2007; published 19 April 2007)

The intrinsic factor to dominate the size-dependent properties of nanocrystals was investigated through applying cohesive energy to determine the physical-chemical properties. With understanding of the nature of the factor, a model for size-dependent melting temperature, Debye temperature, diffusion activation energy, and vacancy formation energy of nanocrystals was established. The accuracy of the developed model was verified by using the available experimental data of gold nanocrystals. It was found that the above properties have the same size-dependent trend which is contributed by the essential effects of surface/volume ratio. The study reveals that the vacancy formation determined by the cohesive energy is the intrinsic factor to dominate the size-dependent physical-chemical properties.

DOI: 10.1103/PhysRevB.75.165413 PACS number(s): 61.46.Hk, 65.80.+n

I. INTRODUCTION

When size of the low-dimensional materials decreases to nanoscale range, electronic, magnetic, optic, catalytic, and thermodynamic properties of the materials are significantly changed, having substantial difference from their bulk properties.[1] Owing to the change of the properties, the fabrication of nanostructural materials and device with unique properties in atomic scale has become an emerging interdisciplinary field involving solid state physics, chemistry, biology, and materials science.[1] Understanding the physical and chemical nature behind the new properties is desired for fabricating the materials for practical applications.[1] Gold (Au) nanocrystals, as one of the noble metals with good corrosion resistance, have extremely high stability. They have been widely researched for optical, electronic, catalytic, and biomedical applications.[2] Recently, the melting temperature T_m,[3–7] the Debye temperature Θ_D,[8,9] the diffusion activation energy E_a,[4,10,11] and the vacancy formation energy E_v,[7,12–14] of the Au nanocrystals have attracted enormous attentions due to their scientific and industrial importance. It is believed that understanding of the melting temperature of the low-dimensional solids is beneficial not only to the theoretical exploitation of phase transition, but also to the applications in modern industries. This is because their thermal stability against melting is increasingly becoming one of the major concerns in the upcoming technologies.[1,3–7] The Debye temperature is an essential physical factor to characterize many material properties, such as the thermal power and phase transitions.[8,9] It is suggested that the diffusion coefficient of nanocrystals is greater than that of their counterpart in bulk.[4,10,11] On the other hand, the vacancy formation energy is also a critical parameter to govern the electrical resistivity, coefficient of thermal expansion, specific heat, and self-diffusion coefficient, etc.[12–14] Through the experiments, it was found that T_m,[3,4] Θ_D,[8] and E_a[10] of the isolated Au nanocrystals progressively reduce with the crystal size decreasing. However, up to date there is still no widespread agreement as to the $E_v(\infty)$ for the particular bulk metals (∞ denotes the bulk) although the vacancy formation mechanisms have been studied substantially.[12–14] This is due to the difficulty of producing an extra pure bulk material with diluted thermal vacancies, thus resulting in lack of experimental data.[12–14] In particular, the experimental data of $E_v(r)$ (r is the radius of crystals) in nanoscale is not available due to the complexity of synthesis and measurement for high quality nanomaterials.[12–14] A theoretical method to predict the $E_v(r)$ function is eagerly awaited.

Recently, several theoretical methods have been developed to model the size dependence of the physical and chemical properties, especially for T_m.[15–18] These models could describe the size dependence of the properties in some aspects, proving the considerable references for investigating the mechanism of size effects on the properties. The common feature of these models is starting from the same point—cohesive energy, E_c. However, the role of E_c on the fundamental mechanism of size dependence has not been fully understood. In addition, a consistent assumption and a unified function of size effects on nanocrystals are needed to consider.

In this work, we demonstrated that the E_c determines a number of physical-chemical properties of nanocrystalline materials. Based on this understanding, the size-dependent cohesive energy model was established to investigate the size dependences of T_m, Θ_D, E_a, and E_v. The accuracy of the developed model is verified with the available experimental data of Au nanocrystals. Through the precise modeling, the intrinsic factor which dominates the size dependence of physical-chemical properties is revealed.

II. METHODOLOGY

The profile of Lennard-Jones (LJ) potential is determined by both bond strength, ε, and equilibrium atomic distance, h.[19] Note that E_c is the sum of ε over all the coordinates of the specific atom with coordination z, and $E_c = zN_a\varepsilon/2$ with N_a being the Avogadro constant. Thus, the variation of the potential profile for nanocrystals, which is related to the crystallographic structures and the corresponding transition functions, should be determined by the change of both E_c and h. In this case, the size effects on the physical-chemical

function could be considered to contribute by the changes of E_c and h. As the change of h is usually in the range of 0.1%–2.5% even when $r<10$ nm,[9] the size effect on h can be neglected. Therefore, size dependence of physical-chemical functions could be predicted if the $E_c(r)$ function is available. For example, the size-dependent critical transition temperatures $T_c(r)$ of ferromagnetic, ferroelectric, and superconductive nanocrystals are modeled in a unified form based on the size-dependent $E_c(r)$ function.[20]

Based on Lindemann's criterion[21] for melting, which is valid for both of bulk and nanocrystals,[22,23] the correlations between $T_m(\infty)$, $\Theta_D(\infty)$, and $E_c(\infty)$ could be obtained. In the criterion, a crystal melts when the root of mean square amplitude (rms), σ, of the atoms reaches a certain fraction of h.[21–23] Combining with Einstein's explanation for the low-temperature specific heats of crystals, a simple expression of the relationship between $T_m(\infty)$ and $\Theta_D(\infty)$ could be written in $\Theta_D(\infty)=c[T_m(\infty)/(MV_m^{2/3})]^{1/2}$, where M is the molar atomic or molecular weight, V_m denotes the molar volume of crystals, and c is a constant.[24] Thus, $\Theta_D^2(\infty)\propto T_m(\infty)$. From Lindemann's criterion, $T_m(\infty)\propto E_c(\infty)$ can be obtained.[15,16] Therefore, we have $\Theta_D^2(\infty)\propto T_m(\infty)\propto E_c(\infty)$. It is assumed that this relationship can be extended to the range of nanoscale as a first order approximation.[20] Thus, $\Theta_D^2(r)/\Theta_D^2(\infty)=T_m(r)/T_m(\infty)=E_c(r)/E_c(\infty)$. In general, the relationship between $E_a(\infty)$, $E_v(\infty)$, and $E_c(\infty)$ can also be expressed as $E_v(\infty)\approx E_a(\infty)/2\approx E_c(\infty)/3$ as a first order approximation.[12–14] So, $E_v(r)/E_v(\infty)=E_a(r)/E_a(\infty)=E_c(r)/E_c(\infty)$. It is known that the weaker metal-metal bond generally results in higher probability of the vacancy formation, presenting that the vacancy formation energy $E_v(\infty)$ is naturally proportional to the cohesive energy $E_c(\infty)$.[12–14] If the vacancies with higher concentration exist in a crystal, their contribution to diffusion is significant as the atoms have much higher mobility.[13] Moreover, high vacancy concentrations will result in the instability of the crystal and finally the subsequent occurrence of melting.[13] Thus, $E_v(\infty)\propto E_a(\infty)\propto T_m(\infty)$ is apprehensible.

Moreover, the relationship of the above properties is also determined by a universal energy relation under a simple two-parameter scaling.[25] The core of the universal energy relation is the essential decay of the electron density into vacancy sites, into interstitial regions, into the vacuum from surfaces, or into the vacuum from isolated atoms.[25–27] It described a universal relation between the scaled electron density and the scaled interatomic separation. Based on this relation, the equivalent-crystal theory[26] and the quantum approximate methods[27] were established and used to calculate materials properties. The calculation properties were also in good agreement with the experimental results and first-principles calculations, thus verifying the correlation of $\Theta_D^2(\infty)\propto T_m(\infty)\propto E_v(\infty)\propto E_a(\infty)\propto E_c(\infty)$.[26,27] Although these methods are different from our consideration, they all explained the same correlation of the properties.

Combining the $E_c(r)$ function reported in literature[28] and the above considerations, a universal relation can be expressed as

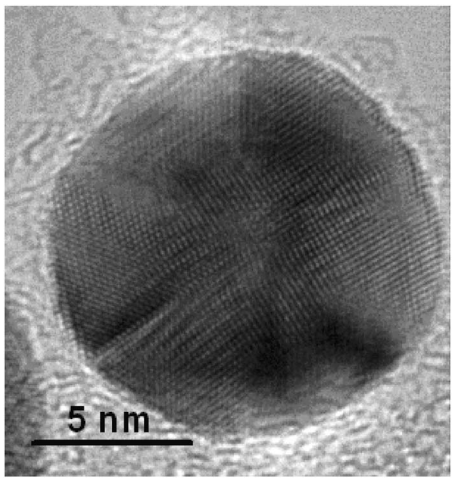

FIG. 1. A high resolution TEM image showing an as-synthesized Au nanoparticle.

$$E_c(r)/E_c(\infty)=T_m(r)/T_m(\infty)=\Theta_D^2(r)/\Theta_D^2(\infty)=E_a(r)/E_a(\infty)=E_v(r)/E_v(\infty)=\left[1-\frac{1}{(4r/h)-1}\right]\exp\left[-\frac{2S_b}{3R}\frac{1}{(4r/h)-1}\right], \quad (1)$$

where $S_b=E_b/T_b$ is the bulk evaporation entropy of crystals with E_b and T_b being the bulk evaporation enthalpy and the evaporation temperature, respectively, and R denotes the ideal gas constant.[28]

III. RESULTS AND DISCUSSION

Au nanocrystals were successfully synthesized by colloids technique. Figure 1 shows a high resolution transmission electron microscope (TEM) image of the as-prepared Au nanoparticle. The modeling result with Eq. (1) is plotted to compare with the experimental and computer simulation results for $T_m(r)$ of Au nanocrystals in Fig. 2. As shown in this figure, $T_m(r)$ decreases with r decreasing, having good agreements between the data even when $r<3$ nm. This exhibits the accuracy of Eq. (1).

Similar comparison between the results obtained from the Eq. (1) and the experimental results for $\Theta_D(r)$ of Au nanocrystals is shown in Fig. 3. It is found that $\Theta_D(r)$ decreases for the isolated nanocrystals as r decreases, which implies an increase in σ since $\sigma^2\propto T/\Theta_D^2$ with T being the absolute temperature.[9] Figure 4 plots $E_a(r)$ of Au nanocrystals which are calculated with Eq. (1) and obtained from experiments, respectively. Other experimental results of $E_a(r)$ for Cu and Fe nanocrystals are also used to verify the model. The results exhibit a good agreement between the calculation and experimental results, as shown in Fig. 4. Since $T_m(r)/T_m(\infty)=E_a(r)/E_a(\infty)$, with Arrhenius relationship of $D(r,T)=D_0\exp[-E_a(r)/(RT)]$ for self-diffusion or intrinsic diffusion (D_0 is the size-independent pre-exponential coefficient),[4,11] we have $D[r,T_m(r)]=D[\infty,T_m(\infty)]$. It implies that the diffusion coefficient at the melting temperature is essentially independent of the crystal size. This result is con-

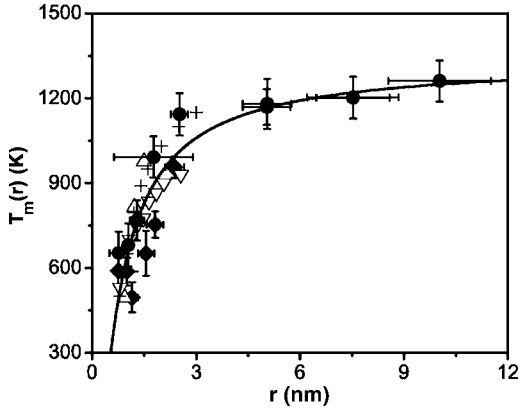

FIG. 2. $T_m(r)$ function of Au nanocrystals. The solid line denotes the consequence of Eq. (1) with $T_m(\infty)=1337.33$ K (Ref. 29), $S_b=E_b/T_b=105.47$ J mol^{-1} K^{-1} as $E_b=330$ kJ mol^{-1} at $T_b=3129$ K (Ref. 29), $R=8.314$ J mol^{-1} K^{-1} and $h=0.2884$ nm (Ref. 30). The symbols ♦ (Ref. 3) and ● (Ref. 4) denote experimental results and △ (Ref. 5), ▽ (Ref. 6), and + (Ref. 7) are computer simulation results from literature.

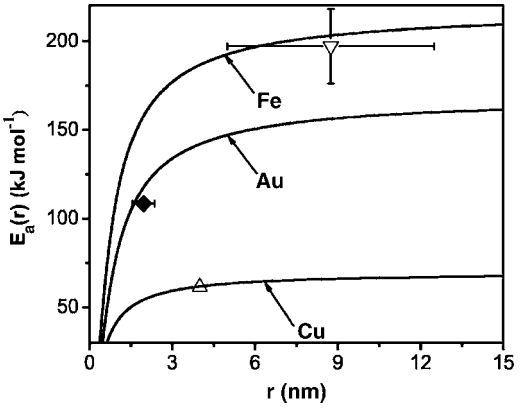

FIG. 4. $E_a(r)$ function of Au, Cu, and Fe nanocrystals. The solid lines denote the consequences of Eq. (1) and the symbols ♦ (Ref. 10), △ (Ref. 31), and ▽ (Ref. 32) are experimental results of Au, Cu, and Fe, respectively. For Au, $E_a(\infty)=168.84$ kJ mol^{-1} (Ref. 33). For Cu, $E_a(\infty)=69.78$ kJ mol^{-1} (Ref. 31), $S_b=E_b/T_b=93.75$ J mol^{-1} K^{-1} as $E_b=300$ kJ mol^{-1} at $T_b=3200$ K (Ref. 29), and $h=0.2238$ nm (Ref. 30). For Fe, $E_a(\infty)=218$ kJ mol^{-1} (Ref. 32), $S_b=E_b/T_b=110.72$ J mol^{-1} K^{-1} as $E_b=347$ kJ mol^{-1} at $T_b=3134$ K (Ref. 29), and $h=0.2483$ nm (Ref. 30).

sistent with recent experimental reports.[4,10] Due to lack of experimental data on $E_v(r)$ function, the only molecular dynamics result of Au nanoparticles[7] is used for comparison with the output of our developed model as shown in Fig. 5. It is discernable that $E_v(r)$ decreases with r decreasing due to the increase of surface/volume ratio and the weakness of the metal-metal bond compared with its counterpart in bulk. From this figure it can be seen that our model has a good agreement with the simulation results. Different from complex and time-consuming computer simulation process, our simple model can also precisely predict value of the size-dependent physical-chemical properties in an explicit analytic expression. All parameters have clear physical meaning in the developed model, which makes it easier to reveal the physical and chemical nature behind the properties.

It is known that the equilibrium vacancy concentration $C_v(r,T)=C_0\exp[-E_v(r)/RT]$ (C_0 is the size-independent pre-exponential coefficient).[13] Thus, $C_v[r,T_m(r)]=C_v[\infty,T_m(\infty)]$ with similar consideration as D. As a result, the equilibrium vacancy concentration at the melting temperature is also independent of the crystal size. Further experimental work will be employed to validate this point. In general, the metallic bonds are weakened when the crystal size is reduced in nanoscale. Since the vacancy formation in solid requires to break bonds between a particular atom and its surrounding atoms, the size reduction makes the vacancy much easier to form.[12–14] It results in the decrease of $E_v(r)$ but increase of C_v. Therefore, the $E_a(r)$ and $T_m(r)$ will decrease due to the increase of C_v.

It is known that the LJ potential is one of the oldest and simplest interatomic pair potentials and has been widely used to model a variety of materials.[19,34] However, the interactions in actual materials are very complex and they are difficult to describe using a simple pair potential. In the past years, the

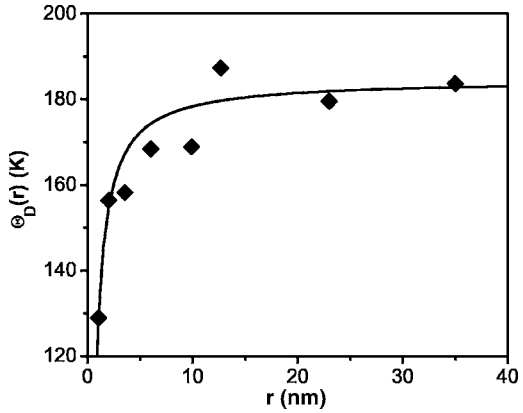

FIG. 3. $\Theta_D(r)$ function of Au nanocrystals. The solid line denotes the consequence of Eq. (1) with $\Theta_D(\infty)=184.59$ K (Ref. 8), and the symbol ♦ (Ref. 8) shows the experimental results.

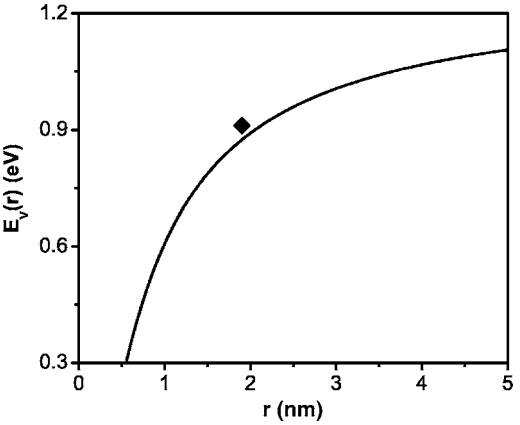

FIG. 5. $E_v(r)$ function of Au nanocrystals. The solid line denotes the consequence of Eq. (1) with $E_v(\infty)=1.27$ eV as $E_c(\infty)=3.82$ eV (Refs. 12–14 and 29), and the symbol ♦ denotes the computer simulation result where an average radius $r=1.9$ nm is used (r is ranged from 0.8 nm to 3 nm) (Ref. 7).

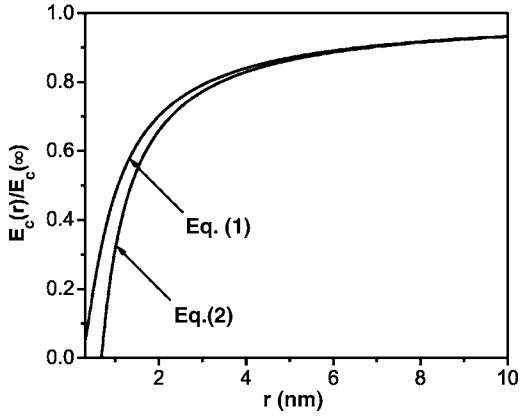

FIG. 6. A comparison between Eqs. (1) and (2). The two solid lines denote the model outputs from Eqs. (1) and (2).

embedded-atom method (EAM) has been developed, which extends a short-range LJ potential into the many-body regime.[34] With the use of this many-body potential, a variety of materials properties can be well described, especially for metals and alloys. However, it is a semi-empirical method, and a comprehensive model is needed to explore and establish for understanding the subtleties of bonding in nanometer scale. Note that both the LJ potential and the EAM have a similar nature in analyzing the basic features of bonding.[34] Therefore, with the understanding of bonding behaviors in nanometer scale, more size-dependent properties of nanocrystals can be calculated and more accurate potentials will be developed to model the interactions and properties of the actual materials.

As a general rule, $\exp(-x) \approx 1-x$ when x is small enough. In such a case, r is at least ten times that of h, or $r>3$ nm. With the first order approximation, Eq. (1) can be rewritten as

$$E_c(r)/E_c(\infty) \approx 1 - \left[S_b/(6R) + \tfrac{1}{4}\right]h/r. \qquad (2)$$

Equation (2) obeys thermodynamic rule of low dimensional materials which the alternation of size-dependent quantity is associated to the surface/volume ratio, or $1/r$.[15–18] This further supports the notion that the discussed physical-chemical properties are most likely affected by the severe bond dangling which is induced by the crystal size reduction in nanoscale. The consequences of Eqs. (1) and (2) for the $E_c(r)/E_c(\infty)$ of Au nanocrystal are plotted in Fig. 6 for comparison. It is discernable that the results from these two models are overlapped when $r>5$ nm while they start to separate when $3<r<5$ nm. When the crystal size is smaller than 3 nm, the outputs from Eqs. (1) and (2) have remarkable differences. It implies that the size effect of the physical-chemical property described by Eq. (1) is weaker than that of Eq. (2). This is because the energetic state of interior atoms of nanocrystals for the smaller crystals is higher than that of the corresponding bulk crystals. Recent experimental results of $T_m(r)$ of indium nanocrystals also validate this point.[35] Equation (2), or $1/r$ correlation mechanism, considers that the physical properties of interior atoms are the same with that of the corresponding bulk crystal, and the depression of physical-chemical properties may be induced solely by the increase of surface atoms percentage as r decreases.[22,23] In fact, similar to the surface atoms, σ of the interior atoms also increases with the decreasing of r, which becomes evident when the size of the nanocrystals is in the mesoscopic size range.[22,23] On the other hand, the nonlinearity correlation in Eq. (1) comes from an essential assumption that the ratio of σ of surface atoms of nanocrystals and that of the atoms within the nanocrystals is size-independent.[22,23] As a result, the interior atoms of nanocrystals have contribution on the size effects, which weaken the vibration effect of surface atoms, thus modifying the physical-chemical properties. It is noted that the thermodynamics has a statistic mechanics basis. When $r<1\sim1.5$ nm, the nanocrystals consist of only several ten to hundred of atoms, the statistic meaning is no longer valid. In addition, the crystalline structure becomes unstable due to its big bond deficit where a cluster with special structure arises. In this case, the disappearance of long-range ordering in the nanocrystals results in different bond structures from the corresponding crystals. This has been well demonstrated by the observation of a unique red-shifted visible emission in ZnO nanoparticles with a radius of 1.5 nm.[36] This is different from the blue-shift of photoluminescence caused by the band gap broadening due to the size reduction in nanometer scale. It is believed that the increase of broken bonds causes localized structural distortion or variation. This is outside the scope of our model description since the developed models are only suitable for crystalline structural materials based on the consideration of a continuous medium.

IV. CONCLUSIONS

In summary, an intrinsic factor that dominates the size-dependent physical-chemistry properties has been investigated through the modeling with modifying the role of cohesive energy. The results of $T_m(r)$, $\Theta_D(r)$, $E_a(r)$, and $E_v(r)$ obtained from the developed models with the data of Au nanocrystals have a good agreement with the experimental results, demonstrating the accuracy of the developed model. Through the modeling, it has been identified that the vacancy formation determined by the cohesive energy is the intrinsic factor to dominate the size-dependent physical-chemical properties. On the other hand, our model could precisely describe the physical-chemical behaviors of the nanocrystals in a very wide span of size range. However, it would be lapse when the long-range ordering no longer exists.

ACKNOWLEDGMENTS

This project is financially supported by Australia Research Council Discovery Program (Grant No. DP0666412).

*Author to whom correspondence should be addressed. Electronic address: ccyang@unsw.edu.au

[1] H. Gleiter, Acta Mater. **48**, 1 (2000).
[2] M.-C. Daniel and D. Astruc, Chem. Rev. (Washington, D.C.) **104**, 293 (2004).
[3] T. Castro, R. Reifenberger, E. Choi, and R. P. Andres, Phys. Rev. B **42**, 8548 (1990).
[4] K. Dick, T. Dhanasekaran, Z. Zhang, and D. Meisel, J. Am. Chem. Soc. **124**, 2312 (2002).
[5] F. Ercolessi, W. Andreoni, and E. Tosatti, Phys. Rev. Lett. **66**, 911 (1991).
[6] L. J. Lewis, P. Jensen, and J.-L. Barrat, Phys. Rev. B **56**, 2248 (1997).
[7] J.-H. Shim, B.-J. Lee, and Y. W. Cho, Surf. Sci. **512**, 262 (2002).
[8] G. Kästle, H.-G. Boyen, A. Schröder, A. Plettl, and P. Ziemann, Phys. Rev. B **70**, 165414 (2004).
[9] C. C. Yang, M. X. Xiao, W. Li, and Q. Jiang, Solid State Commun. **139**, 148 (2006).
[10] T. Shibata, B. A. Bunker, Z. Zhang, D. Meisel, C. F. Vardeman II, and J. D. Gezelter, J. Am. Chem. Soc. **124**, 11989 (2002).
[11] Q. Jiang, S. H. Zhang, and J. C. Li, J. Phys. D **37**, 102 (2004).
[12] T. Korhonen, M. J. Puska, and R. M. Nieminen, Phys. Rev. B **51**, 9526 (1995).
[13] Y. Kraftmakher, Phys. Rep. **299**, 79 (1998).
[14] C. J. Zhang and A. Alavi, J. Am. Chem. Soc. **127**, 9808 (2005).
[15] C. Q. Sun, Prog. Mater. Sci. **48**, 521 (2003).
[16] K. K. Nanda, S. N. Sahu, and S. N. Behera, Phys. Rev. A **66**, 013208 (2002).
[17] G. Guisbiers and M. Wautelet, Nanotechnology **17**, 2008 (2006).
[18] W. H. Qi, M. P. Wang, M. Zhou, and W. Y. Hu, J. Phys. D **38**, 1429 (2005).
[19] J. E. Lennard-Jones, Proc. R. Soc. London, Ser. A **106**, 463 (1924).
[20] C. C. Yang and Q. Jiang, Acta Mater. **53**, 3305 (2005).
[21] F. A. Lindemann, Z. Phys. **11**, 609 (1910).
[22] F. G. Shi, J. Mater. Res. **9**, 1307 (1994).
[23] Q. Jiang, H. X. Shi, and M. Zhao, J. Chem. Phys. **111**, 2176 (1999).
[24] J. G. Dash, Rev. Mod. Phys. **71**, 1737 (1999).
[25] J. H. Rose, J. Ferrante, and J. R. Smith, Phys. Rev. Lett. **47**, 675 (1981); J. H. Rose, J. R. Smith, F. Guinea, and J. Ferrante, Phys. Rev. B **29**, 2963 (1984), and references therein.
[26] J. R. Smith, T. Perry, A. Banerjea, J. Ferrante, and G. Bozzolo, Phys. Rev. B **44**, 6444 (1991).
[27] G. Bozzolo, J. E. Garcés, R. D. Noebe, and D. Farías, Nanotechnology **14**, 939 (2003).
[28] Q. Jiang, J. C. Li, and B. Q. Chi, Chem. Phys. Lett. **366**, 551 (2002).
[29] http://www.webelements.com/
[30] H. W. King, in *Physical Metallurgy*, 3rd ed., R. W. Cahn and P. Haasen, editors (Amsterdam, North-Holland, 1983), pp. 59–63.
[31] J. Horváth, R. Birringer, and H. Gleiter, Solid State Commun. **62**, 319 (1987).
[32] Z. B. Wang, N. R. Tao, W. P. Tong, J. Lu, and K. Lu, Acta Mater. **51**, 4319 (2003).
[33] R. C. Weast, *CRC Handbook of Chemistry and Physics*, 69th ed. (CRC Press, Boca Raton, FL, 1988–1989), pp. F49–52.
[34] M. S. Daw and M. I. Baskes, Phys. Rev. Lett. **50**, 1285 (1983); Phys. Rev. B **29**, 6443 (1984); M. S. Daw, S. M. Foiles, and M. I. Baskes, Mater. Sci. Rep. **9**, 251 (1993).
[35] M. Dippel, A. Maier, V. Gimple, H. Wider, W. E. Evenson, R. L. Rasera, and G. Schatz, Phys. Rev. Lett. **87**, 095505 (2001).
[36] Y. Y. Tay, S. Li, C. Q. Sun, and P. Chen, Appl. Phys. Lett. **88**, 173118 (2006).